

# Headspace Solid-Phase Microextraction

Zhouyao Zhang and Janusz Pawliszyn\*

Department of Chemistry and Waterloo Centre for Groundwater Research, University of Waterloo, Waterloo, Ontario, Canada N2L 3G1

Headspace solid-phase microextraction is a solvent-free sample preparation technique in which a fused silica fiber coated with polymeric organic liquid is introduced into the headspace above the sample. The volatilized organic analytes are extracted and concentrated in the coating and then transferred to the analytical instrument for desorption and analysis. This modification of the solid-phase microextraction method (SPME) shortens the time of extraction and facilitates the application of this method to analysis of solid samples. The detection limits of the headspace SPME technique are at ppt level when ion trap mass spectrometry is used as the detector and are very similar to that of the direct SPME technique. A simple one-dimensional kinetic model has been developed to study the diffusion process involved in headspace SPME. The results from theoretical modeling are consistent with the experimental data. In the experiments, a group of organic compounds, benzene, toluene, ethylbenzene, and xylenes (BTEX), and several polynuclear aromatic hydrocarbons (PAHs) in water were analyzed by the headspace SPME technique. The sampling time for BTEX was reduced to about 1 min compared to about 5 min for direct SPME sampling of the aqueous phase. At ambient temperature, the headspace SPME technique can be used very effectively to isolate compounds with Henry's constants above 90 atm·cm<sup>3</sup>/mol (*i.e.*, three-ring PAHs or more volatile analytes) and can also be used to sample less volatile compounds if high sensitivity can be achieved without reaching equilibrium. The equilibration time for less volatile compounds can be shortened significantly by agitation of both aqueous phase and headspace, reduction of headspace volume, and increase in sampling temperature.

## INTRODUCTION

The analysis of organic contaminants in air, water, and soil has become more and more important because of ever-increasing environmental concerns. The development of simple, efficient, and inexpensive analytical methods are crucial for monitoring and evaluating the environment. The most commonly used techniques for analyzing organic contaminants, such as headspace, purge-and-trap, liquid-liquid extraction, solid-phase extraction, and many others, are effective but have their limitations.<sup>1-4</sup> It is always desirable

to develop new techniques that have the advantages of the old techniques and provide new features. Recently, a novel analytical technique, solid-phase microextraction (SPME), has been developed in our laboratory.<sup>5-11</sup>

The SPME method uses a fine bare fused silica fiber or a fine silica fiber coated with a thin layer of a selective coating (can be solid or liquid) to extract organic compounds directly from aqueous samples for instrumental analysis by gas chromatography (GC) or GC/mass spectrometry (GC/MS).<sup>5-11</sup> The principle behind SPME is the equilibrium partition process of the analyte between the fiber coating and the aqueous solution. For a liquid coating, the amount absorbed by the coating can be calculated from the equation

$$n = C_0 V_1 V_2 K / (K V_1 + V_2) \quad (1)$$

where  $n$  is the mass absorbed by the coating;  $V_1$  and  $V_2$  are the volumes of the coating and aqueous solution, respectively;  $K$  is the partition coefficient of the analyte between the coating and water;  $C_0$  is the initial concentration of the analyte in the aqueous solution. The time efficiency, portability, precision, and detection limit as well as low cost of the SPME technique have been significantly improved in comparison to traditional solid-phase extraction.

For compounds that have a large coating/aqueous partition coefficient, however, the sampling time could be relatively long because of a thin, static layer of water surrounding the fiber coating. This static water layer is extremely difficult to eliminate, even when the aqueous solution is stirred rapidly. The large partition coefficient of the analyte between the coating and the aqueous phase means that more analyte molecules have to pass through this thin static water layer, with a very low diffusion coefficient, to reach the coating. One way to address this kinetic limitation is to use more efficient agitation techniques such as sonication, but this approach requires specialized instrumentation which is quite expensive. In this paper, we have also demonstrated that extraction times can be substantially reduced by sampling analytes indirectly from the headspace above the sample instead of sampling directly from the aqueous solution, because the diffusion of analytes in the vapor phase is 4 orders of magnitude higher than in the aqueous phase. A rapid equilibrium between aqueous and vapor phases can be achieved by constantly stirring the aqueous sample to generate a continuously fresh surface. More importantly, by sampling from the headspace, we also extend the SPME technique to more complex samples which contain solid or high molecular weight materials such as soil and sludge.

\* To whom the correspondence should be addressed.

(1) Novak, J.; Drozd, J. *Instrumentation in Analytical Chemistry*; Zyka, J., Ed.; Ellis Horwood: West Sussex, England, 1991; Vol. 1, Chapter 10.

(2) U.S. EPA method 624 *Fed. Regist.* 1984, 49, 141.

(3) Ho, J. S.; Hodakovic, P.; Bellar, T. A. *Am. Lab.* 1989, July, 14.

(4) Doherty, L. *Am. Environ. Lab.* 1991, 6, 11.

(5) Arthur, C. L.; Pawliszyn, J. *Anal. Chem.* 1990, 62, 2145.

(6) Louch, D.; Motlagh, S.; Pawliszyn, J. *Anal. Chem.* 1992, 64, 1187.

(7) Arthur, C. L.; Killam, L.; Motlagh, S.; Lim, M.; Potter, D.; Pawliszyn, J. *Environ. Sci. Technol.* 1992, 26, 979.

(8) Hawthorne, S.; Miller, D. J.; Pawliszyn, J.; Arthur, C. L. *J. Chromatogr.* 1992, 603, 185.

(9) Arthur, C. L.; Killam, L. M.; Buchholtz, K. D.; Pawliszyn, J.; Burg, J. R. *Anal. Chem.* 1992, 64, 1960.

(10) Potter, D. W.; Pawliszyn, J. *J. Chromatogr.* 1992, 625, 247.

(11) Arthur, C. L.; Potter, D. W.; Buchholz, K. D.; Motlagh, S.; Pawliszyn, J. *LC-GC* 1992, 10, 656.

Sampling from headspace has been explored extensively for many years.<sup>1,12-14</sup> The technique coupled with GC has been used for analyzing volatile organic compounds in the areas such as food, beverage, clinical biochemistry, plant biology, and environmental monitoring. In the previous headspace technique, the enrichment of trace compounds is usually carried out by a precolumn or a liquid nitrogen-cooled trap; the trapped compounds are then purged into GC column for analysis. For concentrated samples, a gas-tight syringe is usually used for sampling the gas sample. The sampling process sometimes involves large and expensive equipment when using the purge-and-trap technique, or a single sample may require several GC runs when using the standard addition method. Another major problem is that the sampling device is nonselective for compounds in the gas phase. In the case of syringe sampling, oxygen and moisture are often injected into the GC column, resulting in the reduction of the column lifetime. There are also problems with adsorption of some analytes in the internal wall of the syringe.

The application of the SPME device for headspace sampling can eliminate all of these problems in the previous headspace techniques and can also extend the headspace sampling to less volatile compounds due to the concentration effect at the fiber coating. In this paper, the equilibrium and kinetics of this new sampling concept are evaluated theoretically and experimentally.

## THEORY

Though the headspace SPME technique can be used for analyzing organic compounds in various matrices and the fiber coating can be solid or liquid, its equilibrium theory and kinetic theory can be better understood by examining a three-phase system in which a liquid polymeric coating, a headspace, and an aqueous solution are involved. The amount of analytes absorbed by the liquid polymeric coating is related to the overall equilibrium of analytes in the three-phase system. Since the total amount of an analyte should be the same during the extraction, we have

$$C_0V_2 = C_1^\infty V_1 + C_2^\infty V_2 + C_3^\infty V_3 \quad (2)$$

where  $C_0$  is the initial concentration of the analyte in the aqueous solution;  $C_1^\infty$ ,  $C_2^\infty$ , and  $C_3^\infty$  are the equilibrium concentrations of the analyte in the coating, the aqueous solution, and the headspace, respectively;  $V_1$ ,  $V_2$ , and  $V_3$  are the volumes of the coating, the aqueous solution, and the headspace, respectively. If we define coating/gas partition coefficients as  $K_1 = C_1^\infty/C_3^\infty$  and gas/water partition coefficient as  $K_2 = C_3^\infty/C_2^\infty$ , the amount of the analyte absorbed by the coating (*i.e.*, the capacity of the coating),  $n = C_1^\infty V_1$ , can be expressed as

$$n = \frac{C_0 V_1 V_2 K_1 K_2}{K_1 K_2 V_1 + K_2 V_3 + V_2} \quad (3)$$

The chemical potential of an analyte in the headspace can be expressed as

$$\mu_v = \mu^0(T) + RT \ln(p_v/p^0) \quad (4)$$

where  $\mu_v$  is the chemical potential of the analyte in the headspace;  $p_v$  is the vapor pressure of the analyte in the headspace;  $\mu^0(T)$  is the chemical potential of the analyte at standard pressure  $p^0$  (usually set  $p^0 = 1$  atm) and temperature

$T$ . Meanwhile, the chemical potentials of the analyte in the coating and the aqueous solution can be expressed as<sup>15</sup>

$$\mu_f = \mu^0(T) + RT \ln(p_f/p^0) \quad (5)$$

$$\mu_w = \mu^0(T) + RT \ln(p_w/p^0) \quad (6)$$

where  $\mu_f$  and  $\mu_w$  are the chemical potentials of the analyte in the coating and the aqueous solution, respectively;  $p_f$  and  $p_w$  are the vapor pressures of the analyte which are in equilibrium with the analyte in the coating and the aqueous solution, respectively. According to the Henry's law,<sup>15</sup> we have

$$p_f = K_F C_1^\infty \quad (7)$$

$$p_w = K_H C_2^\infty \quad (8)$$

where  $K_F$  and  $K_H$  are Henry's constants of the analyte in the liquid polymer coating and the aqueous solution, respectively. When the three-phase system is at equilibrium, the chemical potentials of the analyte in all three phases must be equal

$$\mu_f = \mu_v = \mu_w \quad (9)$$

From eqs 4–6 and eq 9, we have

$$p_f = p_v = p_w \quad (10)$$

If we assume that the ideal gas law  $p_v V_3 = n_v RT$  ( $n_v$  is the numbers of moles of the analyte in the headspace) is valid for the analyte vapor in the headspace, thus

$$p_v = C_3^\infty RT \quad (11)$$

From eqs 7, 8, 11, and 10, we can easily connect the partition coefficients with Henry's constants:

$$K_1 = \frac{C_1^\infty}{C_3^\infty} = \frac{RT}{K_F} \quad (12)$$

$$K_2 = \frac{C_3^\infty}{C_2^\infty} = \frac{K_H}{RT} \quad (13)$$

In the case of direct SPME sampling from the aqueous solution,<sup>6</sup> we have  $\mu_f = \mu_w$  or  $p_f = p_w$  at the equilibrium. The partition coefficient of the analyte,  $K$ , between the coating and the aqueous solution in eq 1 can be expressed as  $K = C_1^\infty/C_2^\infty = K_H/K_F$  since  $p_f = K_F C_1^\infty$  and  $p_w = K_H C_2^\infty$  (eqs 7 and 8). From eqs 12 and 13, it is obvious that

$$K = \frac{K_H}{K_F} = K_1 K_2 \quad (14)$$

Then, eq 3 can be rewritten as

$$n = \frac{C_0 V_1 V_2 K}{K V_1 + K_2 V_3 + V_2} \quad (15)$$

Comparing with eq 1, we notice that except for the extra term of  $K_2 V_3$ , which is related to the capacity ( $C_3^\infty V_3$ ) of the headspace, the two equations are exactly the same. Both equations describe the mass absorbed by the polymeric coating after equilibrium has been reached. For most of the analytes,  $K_2$  is relatively small (for example, benzene has a  $K_2$  value of 0.26), and sampling from the headspace will not affect the amount absorbed by the coating if the volume of the headspace is much less than the volume of the aqueous solution ( $V_3 \ll V_2$ ). The detection limits of the headspace SPME technique are, therefore, expected to be very similar to those of the SPME technique sampling directly from aqueous samples.

The headspace SPME technique is based on the equilibrium of analytes among the involved phases. Equation 15 gives the mass of analytes absorbed by the liquid polymeric coating

(12) Charalambous, G. *Analysis of Food and Beverages, Headspace Technique*; Academic Press: New York, 1978.

(13) Kolb, B. *Applied Headspace Gas Chromatography*; Heyden: London, 1980.

(14) Ioffe, B. V.; Vitenberg, A. G. *Headspace Analysis and Related Methods in Gas Chromatography*; Wiley: New York, 1984.

(15) Atkins, P. W. *Physical Chemistry*, 1st ed.; W. H. Freeman and Co.: San Francisco, CA, 1978; Chapter 8.

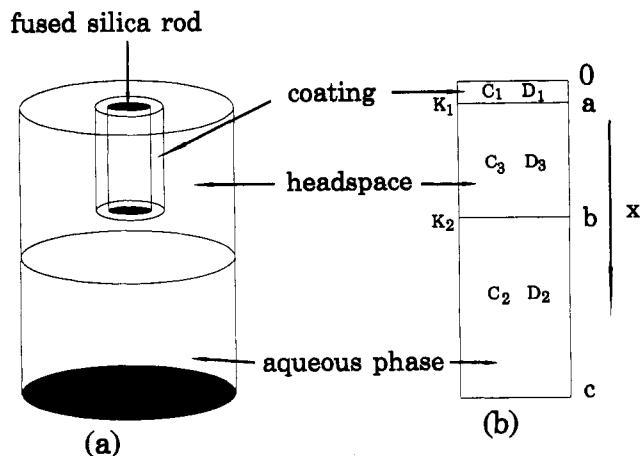


**Figure 1.** (a) Geometry of the real headspace SPME method. (b) One-dimensional model of the three-phase diffusion process;  $K_1$  and  $K_2$  are the coating/gas and gas/water partition coefficients, respectively;  $D_1$ ,  $D_3$ , and  $D_2$  are the diffusion coefficients of the analyte in the coating, the headspace, and water, respectively;  $C_1$ ,  $C_3$ , and  $C_2$  are the concentrations of the analyte in the coating, the headspace, and water, respectively;  $a$ ,  $b-a$ , and  $c-b$  are the thicknesses of the coating, the headspace, and aqueous phase, respectively.

when the equilibrium has been achieved. The kinetics of the mass transport, in which analytes move from the aqueous phase to the headspace and finally to the coating, must also be addressed because it is this process that determines the sampling time of the headspace SPME technique.

The geometry of the SPME headspace extraction is illustrated in Figure 1a. An aqueous sample contaminated with organic compounds is transferred to a closed container with headspace. Chemical equilibrium is allowed to establish between the aqueous solution and the headspace, and then a fused silica fiber coated with a thin layer of a selected liquid organic polymer is inserted into the headspace portion of the container (the fiber does not have any direct contact with the aqueous phase). The fiber's liquid coating starts to absorb organic analytes from the headspace. Analytes undergo a series of transport processes: from water to gas phase and eventually to the coating, until the system finally reaches equilibrium. The diffusion process occurs not only in the axial direction but also in the radial direction as well. Numerical solutions of this diffusion problem can be solved. We are more interested in studying the main factors which control the diffusion process rather than in studying the strict mathematical solutions. A simple one-dimensional diffusion model, as illustrated in Figure 1b, is capable of providing sufficient insight into this diffusion problem. In the model illustrated in Figure 1b, diffusion only occurs in one direction ( $x$ -axis);  $a$  is the thickness of the polymeric coating,  $b-a$  is the length of the headspace; and  $c-b$  is the length of the analyte's aqueous solution. This one-dimensional diffusion process can be described by Fick's second law:

$$\frac{\partial C(x,t)}{\partial t} = D \frac{\partial^2 C(x,t)}{\partial x^2} \quad (16)$$

where  $C(x,t)$  is the concentration of the analyte at position  $x$  and time  $t$ ;  $D$  is the diffusion coefficient of the analyte. The mass of the analyte absorbed by the polymeric coating at any given moment ( $t$ ), can be calculated by

$$M(t) = \int_0^a C(x,t) dx \quad (17)$$

**Modeling of Diffusion Process with Static Aqueous Phase.** In this problem, the diffusion process is governed by eq 16 with the following boundary conditions:

At  $x = 0$ , there is no analyte flowing out of the system, this means

$$\frac{\partial C_1}{\partial x}(x=0,t) = 0 \quad (18)$$

At the interface between the coating and headspace,  $x = a$ , there is a partition of the analyte between two phases

$$C_1(x=a,t) = K_1 C_3(x=a,t) \quad (19)$$

At  $x = b$ , there is a partition between the headspace and the aqueous phase

$$C_3(x=b,t) = K_2 C_2(x=b,t) \quad (20)$$

As shown at  $x = 0$ , at  $x = c$  the analyte cannot flow out of the system

$$\frac{\partial C_2}{\partial x}(x=c,t) = 0 \quad (21)$$

At the interfaces of coating/headspace and headspace/water, the analyte flux must continuously flow through, thus we have

$$D_1 \frac{\partial C_1}{\partial x}(x=a,t) = D_3 \frac{\partial C_3}{\partial x}(x=a,t) \quad (22)$$

and

$$D_3 \frac{\partial C_3}{\partial x}(x=b,t) = D_2 \frac{\partial C_2}{\partial x}(x=b,t) \quad (23)$$

There are also initial conditions: at the beginning of the extraction, the concentration of the analyte in the coating is zero

$$C_1(x,t=0) = 0 \quad (24)$$

If we assume that an aqueous solution with initial concentration of  $C_0$  is transferred into the container and that the equilibrium between the headspace and the aqueous solution has been reached before the SPME extraction, the concentrations in the headspace ( $C_3^0$ ) and in the aqueous solution ( $C_2^0$ ) before the extraction can be calculated through  $C_0(c-b) = C_3^0(b-a) + C_2^0(c-b)$  where  $C_3^0 = K_2 C_2^0$ . Thus, we have two other initial conditions

$$C_2(x,t=0) = C_2^0 \quad (25)$$

$$C_3(x,t=0) = C_3^0 \quad (26)$$

In the above equations,  $D_1$ ,  $D_2$ , and  $D_3$  are the diffusion coefficients of the analyte in the coating, the aqueous phase, and the headspace, respectively, while  $C_1$ ,  $C_2$ , and  $C_3$  are the concentrations of the analyte in the coating, the aqueous phase, and the headspace, respectively;  $K_1$  is the partition coefficient of the analyte between the coating and headspace, and  $K_2$  is the partition coefficient between the headspace and the aqueous phase.

This partial differential equation (eq 16 and its boundary conditions and initial conditions) is very difficult to solve analytically. The finite difference method<sup>16,17</sup> was used here to give the numerical solutions. By applying the so-called "implicit method" of the finite difference, we can express the original partial differential equation and its boundary conditions in a set of equations containing a series of unknown concentrations at various positions of  $x$  at different times. By solving these equations, we can obtain the concentrations of the analyte in any position of  $x$  at any given moment.<sup>18</sup> Using

(16) Riggs, J. B. *An Introduction to Numerical Methods for Chemical Engineers*; Texas Tech University Press: Lubbock, TX, 1988.

(17) Crank, J. *The Mathematics of Diffusion*, 2nd ed.; Clarendon Press: Oxford, U.K., 1989.

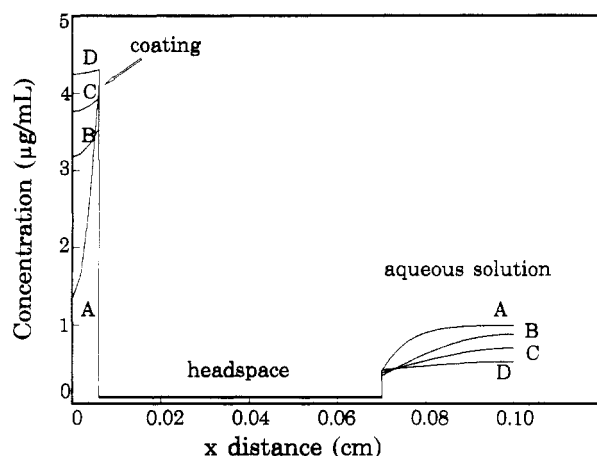


**Figure 2.** Concentration profiles in three phases at different stages of the diffusion process with a static aqueous phase; the parameters used:  $a = 56 \mu\text{m}$ ,  $b = 0.07 \text{ cm}$ ,  $c = 0.1 \text{ cm}$ ,  $K_1 = 50$ ,  $K_2 = 0.2$ ,  $D_1 = 2.8 \times 10^{-6} \text{ cm}^2/\text{s}$ ,  $D_3 = 0.077 \text{ cm}^2/\text{s}$ ,  $D_2 = 1.8 \times 10^{-5} \text{ cm}^2/\text{s}$ ,  $C_0 = 1 \mu\text{g/mL}$ ; (A) at  $t = 3 \text{ s}$ ; (B) at  $t = 15 \text{ s}$ ; (C) at  $t = 30 \text{ s}$ ; (D) at  $t = 60 \text{ s}$ .

eq 17, the time profile of the mass absorbed by the coating can also be calculated.

Figure 2 shows the concentration profiles from  $x = 0$  to  $x = c$  ( $c = 0.1 \text{ cm}$ ) at different extraction times. The small scale of the  $x$ -axis has been chosen in order to show the concentration profiles of all three phases clearly. The parameters used here are related to the poly(dimethylsiloxane) liquid coating with benzene as the analyte. The diffusion coefficients of benzene are as follows: in the coating,  $D_1 = 2.8 \times 10^{-6} \text{ cm}^2/\text{s}$ ; in the headspace,  $D_3 = 0.077 \text{ cm}^2/\text{s}$ ; and in the aqueous solution,  $D_2 = 1.8 \times 10^{-5} \text{ cm}^2/\text{s}$ . The coating thickness  $a = 56 \mu\text{m}$  is used. The thicker the coating, the more the analyte is absorbed by the coating, and *vice versa*; the thickness of the coating will also affect the detection limit of the SPME method. Curve A is the concentration profile in all three phases at the beginning of the extraction ( $t = 3 \text{ s}$ ). As diffusion continues, the concentration in each phase moves gradually toward equilibrium (from curve B to curve D). It can also be noticed that the concentrations in both the coating and aqueous phase vary substantially with distance at the early stage of the extraction while the concentration in the headspace is almost constant along the abscissa. This is because the diffusion coefficient in the headspace is 4 or 5 orders of magnitude higher than those in the other two phases.

As we have indicated at the beginning of this paper, SPME is mainly an equilibration analytical method. The equilibrium of the extraction has been reached when the concentration of the analyte is homogeneous within each of the three phases and the concentration differences between two adjoining phases have satisfied the values of their partition coefficient. In practice, we usually define the equilibrium time as the time at which the mass absorbed by the fiber coating has reached 90% of its final total mass, in other words, at  $t_e$ ,  $M(t_e) = 90\% M(\infty)$ , where  $t_e$  is defined as the equilibration time.

Figure 3 illustrates the time profile of the mass absorbed by the coating at different coating/gas partition coefficient,  $K_1$ , with constant gas/water partition coefficient at  $K_2 = 0.2$ . The values of  $a$ ,  $b$ , and  $c$  used here are closer to the

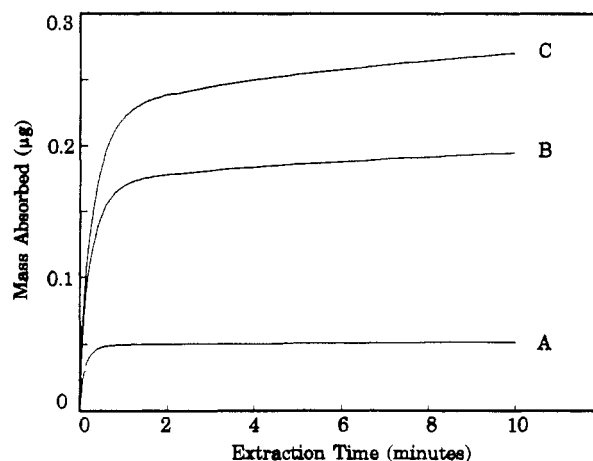


**Figure 3.** Time profile of the mass absorbed by the fiber coating with a static aqueous phase; the parameters used:  $a = 56 \mu\text{m}$ ,  $b = 2 \text{ cm}$ ,  $c = 2.5 \text{ cm}$ ,  $K_2 = 0.2$ ,  $D_1 = 2.8 \times 10^{-6} \text{ cm}^2/\text{s}$ ,  $D_3 = 0.077 \text{ cm}^2/\text{s}$ ,  $D_2 = 1.08 \times 10^{-5} \text{ cm}^2/\text{s}$ ,  $C_0 = 1 \mu\text{g/mL}$ ; (A)  $K_1 = 100$ ; (B)  $K_1 = 1000$ ; (C)  $K_1 = 10000$ .

**Table I. Partition Coefficients of BTEX**

	$K_{ow}$	$K$	$K_1$	$K_2$	$K_H (=K_2RT)$ ( $\text{atm}\cdot\text{cm}^3/\text{mol}$ )	$K_H$ (ref) ( $\text{atm}\cdot\text{cm}^3/\text{mol}$ )
benzene	135	126	493	0.26	$6.4 \times 10^3$	$5.3 \times 10^3$
toluene	489	340	1322	0.26	$6.4 \times 10^3$	$5.7 \times 10^3$
ethylbenzene	1412	528	3266	0.16	$4.0 \times 10^3$	$5.7 \times 10^3$
o-xylene	589	654	4417	0.15	$3.6 \times 10^3$	$5.3 \times 10^3$
p-xylene	1510	831	3507	0.24	$5.8 \times 10^3$	$6.7 \times 10^3$

experimental values. When  $K_1$  becomes large, more analytes are absorbed by the coating, but it requires more time to reach the final equilibrium. For  $K_1 = 100$  (curve A), equilibration time ( $t_e$ ) is about 20 s while  $t_e$  is several hours for  $K_1 = 10000$  (curve C). The long equilibration time in the case of large  $K_1$  is caused by the very slow diffusion of analyte molecules in the aqueous phase. Though the diffusion coefficient in the coating is actually smaller than that in the aqueous phase, the thickness of the coating is usually so small as compared with the other two phases that the diffusion within the coating consumes little time. An interesting phenomenon is that there is a turning point during the extraction process, as shown in Figure 3. The mass absorbed by the coating increases rapidly at the beginning and then slowly levels off. If we designate  $t_T$  as the time needed to reach the turning point, for  $K_2 = 0.2$  and  $K_1 = 100$  (curve A), 90% of the total mass has been absorbed by the coating at the turning point (i.e.,  $t_T = t_e$ ); however, less than 70% of total mass has been absorbed by the coating at  $t_T$  when  $K_2 = 0.2$  and  $K_1 = 10000$  (curve C). Though the values of  $K_1$  changed considerably,  $t_T$  varied very little, from about 20 s for  $K_1 = 100$  to about 60 s for  $K_1 = 10000$ .

These results suggest that in some cases, the mass absorbed by the fiber coating has reached the defined equilibrium [90% of  $M(\infty)$ ] at the turning point. In these cases, the headspace extraction method can be used very effectively, even with a static aqueous phase. The turning point is caused by the rapid diffusion process in the headspace and the very slow diffusion in the aqueous phase. One of the major features of the SPME is that the volume of the fiber coating is extremely small, approximately  $10^{-4} \text{ cm}^3$ . For volatile analytes, like benzene, which has a relatively small  $K_1$  value (thus small  $K$  values in eq 15 since  $K_1 \gg K_2$  for most organic compounds) and relatively large  $K_2$  values (refer to Table I for  $K_1$ ,  $K_2$ , and  $K$  values), the amount of analyte extracted by the coating is insignificant compared to the amount of analyte existing in the headspace. Thus, the concentration in the aqueous solution is virtually unchanged during the extraction. As a

(18) For detailed mathematical derivation, please refer to the Appendix in ref 6.

(19) Newns, A. C.; Park, G. S. *J. Polym. Sci.: Part C* 1969, 22, 927.

(20) Washburn, E. W. *International Critical Tables of Numerical Data, Physics, Chemistry and Technology*; McGraw-Hill: New York, 1926; Vol. 5, p 62.

(21) Wendt, J. O. L.; Frazler, G. C., Jr. *Ind. Eng. Chem. Fundam.* 1973, 12, 239.

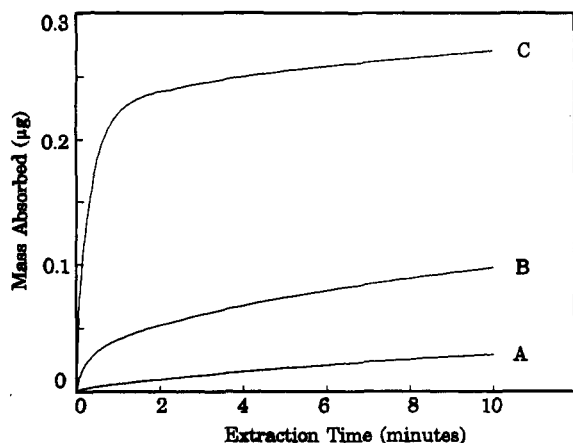


Figure 4. Time profile of the mass absorbed by the fiber coating with a static aqueous phase. The values of  $a$ ,  $b$ ,  $c$ ,  $D_1$ ,  $D_2$ ,  $D_3$ , and  $C_0$  are the same as those in Figure 3, but  $K_1 = 10\,000$ ; (A)  $K_2 = 0.2$ ; (B)  $K_2 = 0.02$ ; (C)  $K_2 = 0.002$ .

result, the extraction time is determined largely by diffusion in the vapor phase. The sampling time is quite short.

Figure 4 shows the effect of the gas/water partition coefficient,  $K_2$ , on the extraction. Curves A–C show the time profiles of the mass absorbed by the coating with  $K_2 = 0.002$ ,  $0.02$ , and  $0.2$ , respectively, and  $K_1 = 10\,000$  for all three curves. When the analyte has a small  $K_2$  value (thus, the Henry's constant  $K_H = K_2RT$  is also small), the concentration of the analyte in the headspace is low, the headspace extraction affects the concentration of the aqueous phase, and it takes a very long time to reach equilibrium. As there is less analyte in the headspace, the mass absorbed by the coating is far smaller than  $M(t_e)$  at the turning point.

The above results suggest that if the headspace SPME method is used with a static aqueous phase, analytes should have large Henry's constants which can be the result of high volatility and hydrophobicity of the analytes, and should not have very large partition coefficients between the fiber coating and the headspace. Volatile organic compounds usually meet these requirements; thus, this method can be used to differentiate volatile compounds from less volatile compounds.

**Modeling of Diffusion Process with Well-Agitated Aqueous Phase.** In this case, we consider an ideal situation in which the aqueous phase is perfectly mixed, *i.e.*, the convection in the aqueous solution is infinitely fast and the aqueous phase is always homogenous. In reality, a well-agitated aqueous phase simply means that the mass transport in the aqueous phase is much faster than that in the other two phases and is not a limiting step for the whole diffusion process. This can be achieved by stirring the aqueous solution very rapidly.

Mathematically, the boundary conditions of eq 16 are now different from those used earlier. While eqs 18–20 and 22 are still useful, eqs 21 and 23 are no longer valid. But we also no longer need to know the concentration distribution in the aqueous solution since at a given moment this concentration should be the same everywhere in the aqueous phase, in other words

$$C_2(x, t) = C_2(t) \quad (27)$$

We can derive another equation from the mass balance since at any moment the total mass should always equal the total mass that existed initially

$$\int_0^a C_1(x, t) dx + \int_a^b C_3(x, t) dx + (c-b)C_2(t) = C_3^0(b-a) + C_2^0(c-b) \quad (28)$$

The initial concentration within the fiber coating,  $C_1^0$ , is zero. Equations 27 and 28 can be used to replace eqs 21 and 23. By using the same implicit finite difference method used for

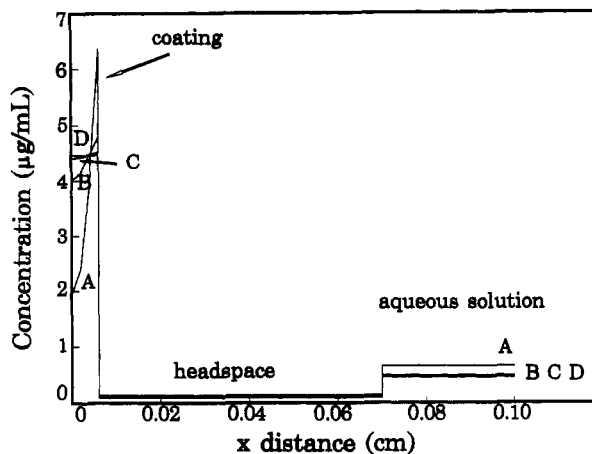


Figure 5. Concentration profiles in three phases at different stages of the diffusion process with a well-agitated aqueous phase; the parameters used:  $a = 56\text{ }\mu\text{m}$ ,  $b = 0.07\text{ cm}$ ,  $c = 0.1\text{ cm}$ ,  $K_1 = 50$ ,  $K_2 = 0.2$ ,  $D_2 = 2.8 \times 10^{-6}\text{ cm}^2/\text{s}$ ,  $D_3 = 0.077\text{ cm}^2/\text{s}$ ,  $C_0 = 1\text{ }\mu\text{g/mL}$ ; (A) at  $t = 3\text{ s}$ ; (B) at  $t = 9\text{ s}$ ; (C) at  $t = 15\text{ s}$ ; (D) at  $t = 21\text{ s}$ .

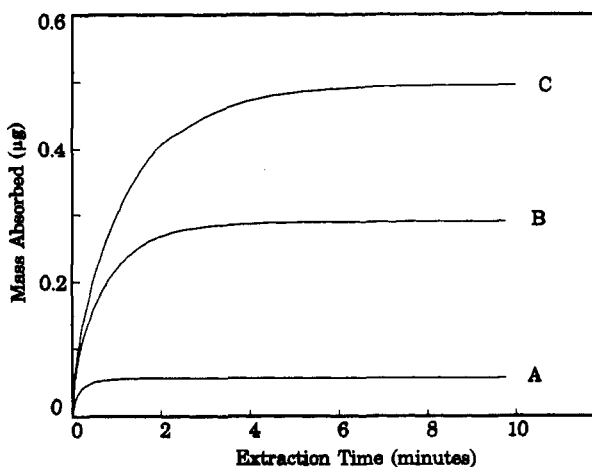
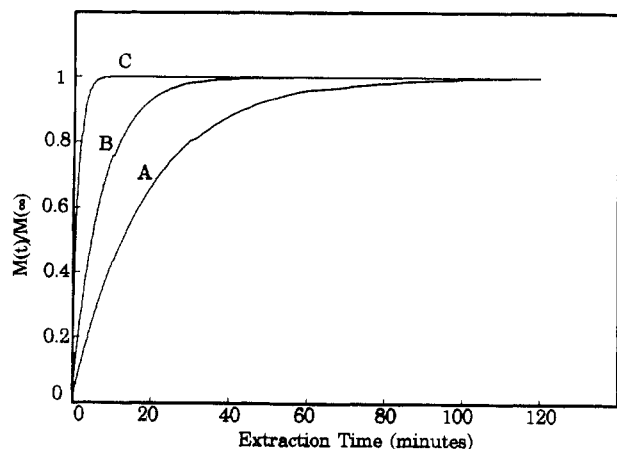


Figure 6. Time profile of the mass absorbed by the fiber coating with an agitated aqueous phase; the parameters used:  $a = 56\text{ }\mu\text{m}$ ,  $b = 2\text{ cm}$ ,  $c = 2.5\text{ cm}$ ,  $K_2 = 0.2$ ,  $D_1 = 2.8 \times 10^{-6}\text{ cm}^2/\text{s}$ ,  $D_3 = 0.077\text{ cm}^2/\text{s}$ ,  $C_0 = 1\text{ }\mu\text{g/mL}$ ; (A)  $K_1 = 100$ ; (B)  $K_1 = 1000$ ; (C)  $K_1 = 10\,000$ .

the static model with the same initial conditions (eqs 24–26), we can get concentrations at any  $x$  value at any moment. Again, through eq 17, the mass absorbed by the coating at any given time can be calculated.

Figure 5 shows the concentration profiles in each of the three phases at different extraction times. The parameters used here have been mentioned previously, except the diffusion coefficient ( $D_2$ ) of the analyte in the aqueous solution is no longer applicable because that phase is under rapid agitation. Compared with Figure 2, the major difference is that the equilibrium can be achieved more quickly. This can be seen by comparing curve D in both figures. Also notice that in Figure 2 curve D is 60 s while in Figure 5 it is 21 s. The initial high concentration at the edge of the coating in Figure 5 (curve A) is caused by the rapid diffusion in the headspace and aqueous phase and the small volumes of these two phases. At the beginning of the extraction, the outer most coating extracts a lot of the analyte from the container, while the analyte does not have enough time to diffuse deep into the coating.

Figure 6 shows the time profile of the mass absorbed by the coating at different values of the coating/gas partition coefficient,  $K_1$ , with constant gas/water partition coefficient,  $K_2 = 0.2$ . The larger the  $K_1$  values, the longer the equilibration time because more analytes need to be transported through the gas phase, which is now the limiting phase. The equilibration time increases from 20 s for  $K_1 = 100$  (curve A)



**Figure 7.** Time profile of the mass absorbed by the fiber coating with an agitated aqueous phase. The values of  $a$ ,  $b$ ,  $c$ ,  $D_1$ ,  $D_3$ , and  $C_0$  are the same as those in Figure 6, but  $K_1 = 10\,000$ ; (A)  $K_2 = 0.2$ ; (B)  $K_2 = 0.02$ ; (C)  $K_2 = 0.002$ .

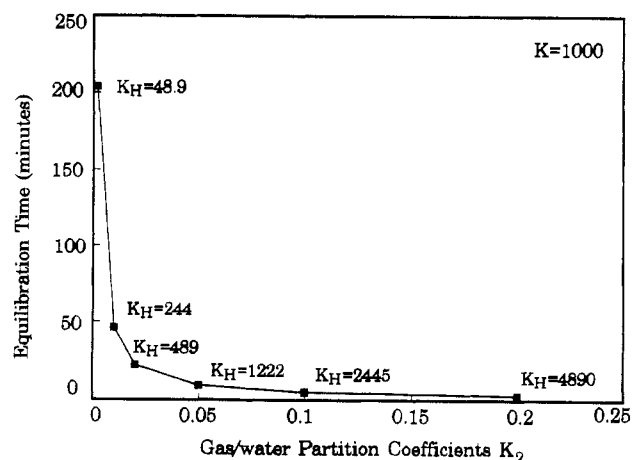
to 130 s for  $K_1 = 10\,000$  (curve C). These results indicate that with a well-agitated aqueous phase and relatively large  $K_2$  values (i.e., the analyte has a relatively large Henry's constant in aqueous solution), the headspace SPME extraction reaches equilibrium in quite a short time even when the partition coefficient between the coating and headspace,  $K_1$ , is very large.

Figure 7 shows the time profile of the mass absorbed (normalized) by the coating at different  $K_2$  values with the same  $K_1$ . The equilibration time becomes longer as Henry's constants of organic compounds become smaller. For  $K_2 = 0.2$  and  $K_1 = 10\,000$  (curve C), the equilibration time is 130 s, while for  $K_2 = 0.002$  and  $K_1 = 10\,000$  (curve A), the equilibration time is about 60 min. Since the aqueous phase is well-agitated and the coating is very thin, the limiting step is now diffusion in the headspace (i.e., from the headspace/water interface to the coating/headspace interface). As Fick's first law points out, the rate of diffusion depends on both the diffusion coefficient and the gradient of the concentration:

$$J = -D \frac{\partial C}{\partial x} \quad (29)$$

where  $J$  is the flux of the analyte. In the headspace, the diffusion coefficients of analytes are relatively large, but the concentrations, thus concentration gradients, become smaller and smaller as Henry's constants decrease if the length of the headspace is unchanged. As a result, the transport of analytes through the headspace is very slow, and it may take quite a long time to achieve the equilibrium.

Figure 8 shows the effect of  $K_2$  on the equilibration time. In the figure, the partition coefficient between the coating and water,  $K = K_1 K_2$ , has been kept the same. When we analyze the aqueous samples contaminated with organic compounds, it is always more convenient to deal with the partition coefficients of analytes between the coating and water instead of  $K_1$  and  $K_2$  since  $K$  values are usually close to  $K_{ow}$  values, the partition coefficient of the analyte between 1-octanol and water.  $K_{ow}$  values can be easily found in the literature for most organic compounds.<sup>22</sup> If  $K$  is kept the same, the larger the  $K_1$ , the smaller the  $K_2$ , and *vice versa*. In the figure, the corresponding Henry's constants (the unit is  $\text{atm}\cdot\text{cm}^3/\text{mol}$ ),  $K_H$ , are also shown. For  $K = 1000$ , when  $K_2 = 0.002$  (which corresponding to Henry's constant  $K_H = 48.9 \text{ atm}\cdot\text{cm}^3/\text{mol}$  at  $T = 298 \text{ K}$ , and  $K_1 = 5 \times 10^6$ ), the equilibration time could be more than 3 h even with a well-agitated aqueous phase. Because of the simplified model, the above results cannot be used to directly determine the equilibration time



**Figure 8.** Equilibration time vs  $K_2$  with  $K = 1000$ . The aqueous phase is well-agitated. The points in the figure are as follows:  $K_2 = 0.2, 0.1, 0.05, 0.02, 0.01$ , and  $0.002$ . The corresponding  $K_H$  values are also indicated. The unit of  $K_H$  is  $\text{atm}\cdot\text{cm}^3/\text{mol}$ .

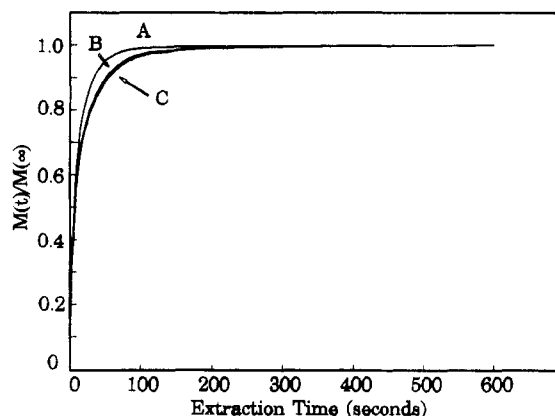


**Figure 9.** Time profile of the mass absorbed by the fiber coating with an agitated aqueous phase. The values of  $a$ ,  $b$ ,  $c$ ,  $D_1$ ,  $D_3$ , and  $C_0$  are the same as those in Figure 6, but  $K_1 = 100$ ; (A)  $K_2 = 0.2$ ; (B)  $K_2 = 0.02$ ; (C)  $K_2 = 0.002$ .

for an analyte in a real experiment, but Figure 8 does provide the important relationship between coating/water partition coefficients ( $K$ ), Henry's constants ( $K_H$ ), and equilibration time.

For compounds that have a coating/water partition coefficient,  $K$ , much smaller than 1000, the equilibration time does not change significantly as the gas/water partition coefficient,  $K_2$ , becomes smaller. In Figure 9,  $K = 20, 2$ , and  $0.2$  as  $K_2$  decreases from  $0.2$  to  $0.002$ , respectively (curves A–C) while the coating/gas partition coefficient,  $K_1$ , is kept at  $100$ . The equilibration times in these three cases differ very little. This is because the amount of the analyte absorbed by the coating is comparable to the capacity of the headspace when  $K$  values are small (refer to eq 15). There is no need for a large amount of analyte to transport from the aqueous phase through the headspace to the coating. Thus, a slow transport rate of less volatile compounds in the headspace does not have a major impact on the equilibration time when  $K$  is small. As  $K$  values become smaller, the mass absorbed by the fiber coating also becomes smaller, which leads to lower sensitivity. For very volatile compounds ( $K_2$  is large), small  $K$  values mean small  $K_1$  values. If the  $K_1$  value is about  $1$ , it means that the fiber coating does not extract analytes effectively. In that case, the headspace syringe injection would be preferable.

## EXPERIMENTAL SECTION

**Apparatus and Reagents.** The SPME device has been described in great detail in previous papers.<sup>5–11</sup> The fiber used

(22) Valko, K.; Papp, O.; Darvas, F. *J. Chromatogr.* 1984, 301, 355.

here was a fused silica rod, its surface was coated with a 56- $\mu\text{m}$  polymeric coating, and the silica rod had an o.d. of 141  $\mu\text{m}$  and a total o.d. (fused silica rod + coating) of 253  $\mu\text{m}$ . This gave the coating a volume of about  $3.4 \times 10^{-4} \text{ cm}^3$  for a 1.0-cm length fiber. The coating material was poly(dimethylsiloxane) (Polymicro Technologies, Tuscon, AZ). At one end of a 1.5-cm fiber, the coating was stripped for about 0.5 cm, while the remaining 1 cm was left coated. The bare end of the fiber was inserted into a stainless steel tubing to give an assembly which was composed of a 21-cm stainless steel tubing with 1-cm fiber at one end. This assembly was then put into a Hamilton 7105 syringe. This device is operated like an ordinary syringe for sampling and injection.

The GC used here was Varian 3500 equipped with a septum-equipped programmable injector (SPI) and a flame ionization detector (FID). This GC was also equipped with cryogenics in both the injector and the column for temperature programming (Varian, Georgetown, ON). The column used was a 30 m  $\times$  0.25 mm DB-5 column with a stationary phase thickness of 0.25  $\mu\text{m}$  (Chromatographic Specialties, Brockville, ON). The injector septum was a LB-2 septa (Supelco, Oakville, ON).

The GC/MS used here was Varian's Saturn I system which included a Varian 3400 GC with an ion trap mass spectrometer. The injector and column in the Varian 3400 is the same as those in the Varian 3500.

The 1.8-mL autosampler vials (Chemical Research Supplies, Oakville, ON) used have a total capacity of about 2.3 mL. For the agitated samples, a 7 mm  $\times$  2 mm magnetic stirbar (Bel-Art Products, Pequannock, NJ) was placed in the sample vial, and the solution was stirred with a magnetic stirrer during the headspace extraction. All chemicals were of ACS grade (BDH, Toronto, ON).

**Procedure.** A 1  $\mu\text{L/mL}$  BTEX/methanol (benzene, toluene, ethylbenzene, and *m,o,p*-xylene commonly known as BTEX) standard solution was prepared by dissolving 10  $\mu\text{L}$  each of benzene, toluene, ethylbenzene, and *m,o,p*-xylenes in 10 mL of methanol at room temperature. A sample of 10  $\mu\text{L}$  of this standard solution was diluted to 10 mL with deionized water to give an approximately 1 ppm BTEX aqueous solution.

A 100  $\mu\text{g/mL}$  toluene solution of several polynuclear aromatic hydrocarbon (PAH) compounds (naphthalene, acenaphthene, phenanthrene, and chrysene) was prepared, and then 1 mL of this solution was transferred into 9 mL of acetone to give a 10  $\mu\text{g/mL}$  solution. Finally, a 250- $\mu\text{L}$  acetone solution was spiked into 25 mL of water to make a 0.1  $\mu\text{g/mL}$  aqueous solution of naphthalene, acenaphthene, phenanthrene, and chrysene. A 10  $\mu\text{g/mL}$  acetone solution of deuterized PAHs, naphthalene-*d*<sub>8</sub>, acenaphthene-*d*<sub>10</sub>, phenanthrene-*d*<sub>10</sub>, and chrysene-*d*<sub>12</sub> was prepared by the same procedure. These deuterized PAHs, purchased from Supelco, Oakville, ON, were used as internal standards.

For the headspace SPME extraction, exactly 0.5 mL of both the BTEX and PAH prepared aqueous solutions were transferred into the sample vials; they were then put on the bench for about 2 h to allow analytes to reach thermal equilibrium between the headspace and aqueous phase before the headspace SPME extraction.

The signals of BTEX from the GC FID detector were calibrated by syringe injections of 0.2  $\mu\text{L}$  of 10 ppm BTEX in dichloromethane. The FID signals of PAHs were calibrated by syringe injections of 0.2  $\mu\text{L}$  of 10  $\mu\text{g/mL}$  PAHs/acetone solution.

An internal standard was used for the analysis of the PAH-contaminated sewage and soil samples. A 0.2- $\mu\text{L}$  sample of a standard 10  $\mu\text{g/mL}$  acetone solution of PAH and deuterized PAH was injected into GC/MS to give the response factor of the MS signal. A 0.2- $\mu\text{L}$  sample of a 10  $\mu\text{g/mL}$  deuterized PAH (used as internal standard) acetone standard solution was spiked into a 0.5-mL PAH-contaminated sewage sample to give a deuterized PAH concentration of 4.0 ng/mL, i.e., about 4 ppb. A total of 0.1 mL of the same deuterized PAH standard solution was spiked into a 1.0-g PAH-contaminated soil sample to give a deuterized PAH concentration of 1  $\mu\text{g/g}$  or 1 ppm.

During the headspace extraction, the fused silica fiber coated with poly(dimethylsiloxane) was drawn into the needle of the syringe, and the needle was used to penetrate the septum of a sealed sample vial. The fiber was then lowered into the headspace by depressing the plunger for a predetermined time. The fiber within the vial stayed above the aqueous phase and never contacted the aqueous solution. Once the sampling was finished,

the fiber was immediately inserted into the GC injector for desorption. The desorption time of the fiber within the GC injector was set at 1 min for BTEX and 2 min for PAH contaminated samples including sewage and soil samples.

A 500-mL BTEX gas sample was prepared by injecting 2  $\mu\text{L}$  each of benzene, toluene, ethylbenzene, and *m,o,p*-xylene into a 500-mL gas standard bottle. A 2.5-mL gas-tight syringe was used to inject exactly 0.5 mL of the prepared gas sample directly into GC. The results were compared with those from the SPME extraction of the same gas sample. The partition coefficients of the BTEX between the polymeric coating and the gas phase were calculated using

$$K_1 = \frac{A_F V_G}{A_G V_F} \quad (30)$$

where  $A_F$  and  $A_G$  were the peak areas from the GC corresponding to the fiber coating injection and direct gas injection, respectively;  $V_F$  was the volume of the coating; and  $V_G$  was the volume of the gas sample injected. The  $K_1$  data reported in Table I were the average values of three measurements. All SPME extractions mentioned above were carried out at room temperature.

The GC method for BTEX<sup>6,7</sup> is as follows: the fiber was desorbed in the GC injector at 150 °C for 1 min; the GC column was maintained at -5 °C for 2 min and then ramped to 150 °C at a rate of 15 °C/min. The GC method for PAHs is as follows: the fiber coating was desorbed in the GC injector at 300 °C for 2 min; the GC column was maintained at 60 °C for 1 min at the beginning of the GC run and then the column temperature was ramped to 280 °C at a rate of 15 °C/min; the column was maintained at 280 °C for 5 min and then ramped to 300 °C at a rate of 20 °C/min. The total time of a single GC run was 21.66 min. The temperature of FID detector was 300 °C.

## DISCUSSIONS OF EXPERIMENTAL RESULTS

The partition coefficient between the coating and aqueous phase,  $K$ , is related to  $K_1$  (partition coefficient of coating/headspace) and  $K_2$  (partition coefficient of headspace/aqueous phase) through  $K = K_1 K_2$  (eq 14).  $K$  values for BTEX have been measured in previous work.<sup>6,7</sup> By measuring  $K_1$ , we can get  $K_2$  (or Henry's constants  $K_H = K_2 RT$ ). Henry's constants of BTEX can also be found in the literature.<sup>23-25</sup> Table I lists the important partition coefficients of BTEX.  $K_{ow}$  is the partition coefficient of an analyte between octanol and water.<sup>22</sup> Values of  $K_1$  were measured by the method described in the experimental section, and  $K_2$  values were calculated ( $K_2 = K/K_1$ ) as were  $K_H$  values ( $K_H = K_2 RT$ , where  $T$  is the ambient temperature, 298 K).  $K_H(\text{ref})$  values were found in the literature.<sup>23-25</sup> From Table I, it is quite clear that the Henry's constants measured experimentally using the SPME technique and those reported by the literature are very close. This indicates the validity of the relationship of  $K = K_1 K_2$  in the headspace SPME method. Thus, this method, based on the multiphase equilibration principle, has a solid theoretical base. It is also worth pointing out that some basic physical constants of analytes, polymeric coatings, and aqueous solutions may be measured with reasonable accuracy using the SPME method. We have demonstrated one example in Table I—the measurement of the Henry's constants. The successful measurements of the Henry's constants also indicate that sampling the organic contaminants from a pure gas phase by the SPME technique can be used very effectively. The SPME technique shows the potential to provide a new way to monitor air pollution.

Figure 10 shows the time profile of benzene, toluene, ethylbenzene, *m*-xylene, *o*-xylene, and *p*-xylene (commonly

(23) Callahan, M. *Water-related Environmental Fate of 129 Priority Pollutants*; National Technical Information Service: Springfield, VA, 1979; Vol. 1.

(24) Dean, J. A. *Langes's Handbook of Chemistry*; McGraw-Hill: New York, 1973.

(25) Hansch, C.; Leo, A. *Substituent Constants for Correlation Analysis in Chemistry and Biology*; Wiley-Interscience Publication: New York, 1979.



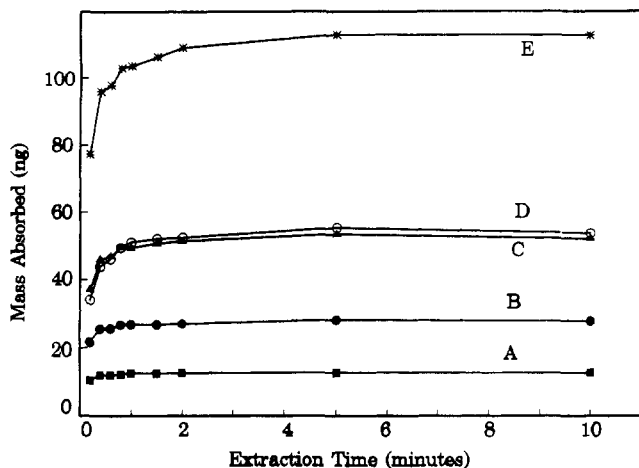


**Figure 10.** Time profile of the mass absorbed by the fiber coating with a 1 ppm initial concentration of BTEX aqueous solution and a well-agitated water phase; (A) benzene, (B) toluene, (C) ethylbenzene, (D) *m,p*-xylene, (E) *o*-xylene.

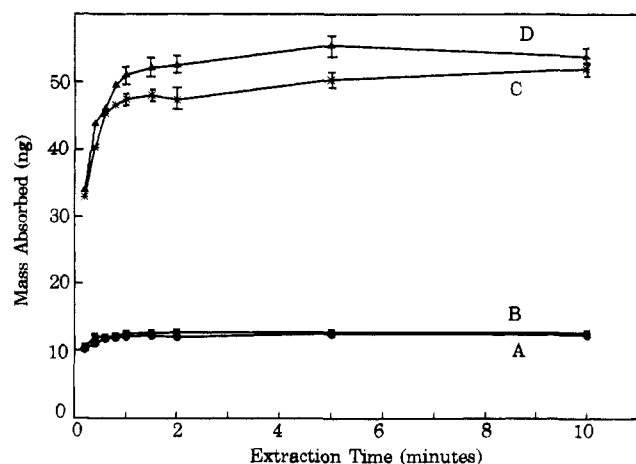


**Figure 11.** Time profile of the mass absorbed by the fiber coating with a 1 ppm initial concentration of benzene and *o*-xylene aqueous solution; (A) benzene with a static aqueous phase; (B) benzene with a well-agitated aqueous phase; (C) *o*-xylene with a static aqueous phase; (D) *o*-xylene with a well-agitated aqueous phase.

known as BTEX) absorbed by the coating. BTEX compounds were sampled by the headspace SPME technique with a stirred aqueous phase (the stirring rate was controlled to be 75% of the maximum stirring rate of the stirrer). The results indicate that the equilibration time for the headspace extraction is very short, approximately 40 s for benzene (curve A) and toluene (curve B), 1 min for ethylbenzene (curve C) and *o*-xylene (curve D), and 2 min for *m*- and *p*-xylene (curve D; these two compounds coelute from the GC column). Compared with the direct SPME sampling from the water,<sup>6</sup> the equilibration times are significantly reduced, for example, the equilibration time of *p*-xylene was reduced from 6 to 2 min. The results in Figure 10 also indicate that the equilibration times depend on partition coefficients. The gas/water partition coefficients,  $K_2$ , for benzene, toluene, and *p*-xylene are similar, thus the larger the coatings/gas partition coefficients,  $K_1$ , the longer the equilibration time as discussed in the theoretical section. For ethylbenzene and *o*-xylene, the difference of their equilibration times can not be resolved in our experiments because their  $K_2$  values are close and their  $K_1$  values do not differ significantly. The dependence of equilibration time on the partition coefficients is very consistent with the theoretical predictions.

Figure 11 compares the results from the samples with agitated aqueous solution and those with static aqueous solution. Curves A and B are the time profiles of benzene with a static and agitated aqueous phase, respectively. Since

**Table II.** Partition Coefficients of Several PAHs

	$\log K_{ow}$	$K_2$ ( $=K_H/RT$ )	$K_H$ ( $\text{atm}\cdot\text{cm}^3/\text{mol}$ )
naphthalene	3.59	0.019	$4.6 \times 10^2$
acenaphthene	4.07	$3.7 \times 10^{-3}$	91
anthracene	4.54	$3.5 \times 10^{-3}$	86
phenanthrene	4.57	$1.6 \times 10^{-3}$	40
benz[a]anthracene	5.9	$4.1 \times 10^{-5}$	1.0
chrysene	5.84	$4.3 \times 10^{-5}$	1.05

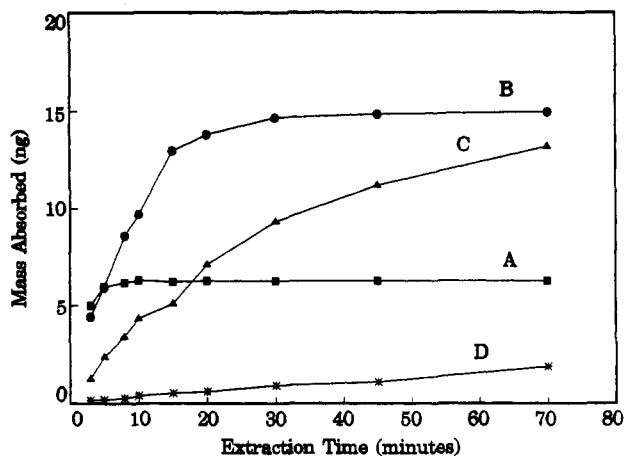
benzene has a relative small  $K_1$  and a large  $K_2$  (refer to Table I), it is not surprising that these two curves are almost identical, as it has been suggested in the theoretical section: the agitation of the aqueous phase is not going to make a big difference on the equilibration time for compounds with large  $K_2$  values and small  $K_1$  values, like benzene, because of a large headspace capacity for such compounds. However, the agitation makes a significant difference for *o*-xylene, which has a quite large  $K_1$ , as shown in curves C and D. The equilibration time (curve D) is about 1 min for the well-agitated sample, while it takes much longer time for the nonagitated sample (curve C) to reach equilibrium. Curves A and C are both from the nonagitated sample, but the equilibration times differ significantly because of their large differences in partition coefficients. When compounds with even smaller Henry's constants are analyzed, it is expected that the effect of the agitation in the aqueous phase will be more significant. This has been discussed in detail in the theoretical section.

The introduction of headspace reduces the amount of analytes absorbed by the coating as indicated in eq 15. In this study, a large headspace/water volume ratio is used because the headspace must accommodate 1-cm silica fiber, and small vials were used. Compared with direct SPME sampling under the same conditions,<sup>6</sup> the amount of analytes absorbed by the coating using headspace SPME is about 50% less. This is not surprising because there is an extra term  $K_2V_3$  in eq 15 compared with the direct sampling eq 1. After the effect of  $K_2V_3$  is taken into consideration, the two results are in fact very consistent. The detection limit of the headspace method will be about twice the limit of the direct SPME sampling because of the headspace volume. The limit of detection can be improved by applying smaller headspace/sample ratio. In the previous study, it has been found that the limit of detection for the SPME technique with an ion trap mass spectrometer is at the parts per trillion (ppt) level<sup>10</sup> and the dynamic linear range is very broad.<sup>7,10</sup>

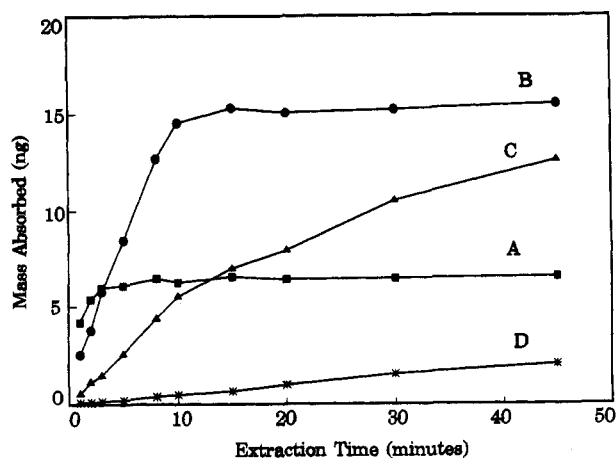
The above results indicate that the headspace SPME technique is very efficient for analyzing volatile organic compounds since they usually have large Henry's constants,  $K_H$ , thus a large  $K_2$ . When  $K_H$  becomes smaller, the equilibration time tends to become longer as suggested in the theoretical section. Semivolatile organic compounds such as polynuclear aromatic hydrocarbons (PAHs) usually have large  $K_{ow}$  values and small  $K_H$  values. Table II lists the partition coefficients of several PAHs.<sup>22-25</sup>  $K_2$  values are calculated from the relationship,  $K_2 = K_H/RT$  with  $T = 298$  K. Compared with BTEX (refer to Table I), these compounds have much smaller  $K_H$  values and much larger  $K_{ow}$  values.

Figure 12 shows the profile of several PAH compounds with a stirred aqueous phase. The stirring is controlled to be 75% of the maximum stirring rate of the magnetic stirrer, which is the same as the stirring rate for BTEX. The equilibration time is about 8 min for naphthalene and 30 min for acenaphthene. Both phenanthrene and chrysene do not reach the equilibrium within 70 min because of their large  $K_{ow}$  and small  $K_H$ . From Table II,  $K_{ow}$  and  $K_H$  values of acenaphthene and phenanthrene do not differ significantly, but their equilibration times have a very big difference. If we refer to Figure 8, it has been predicted by the kinetic theory that a small decrease in Henry's constant,  $K_H$ , will lead to a





**Figure 12.** Time profile of the mass absorbed by the fiber coating with a 0.1 µg/mL (0.1 ppm) initial concentration of PAHs aqueous solution. The aqueous phase is stirred at 75% of the maximum stirring rate; (A) naphthalene; (B) acenaphthene; (C) phenanthrene; (D) chrysene.



**Figure 13.** Time profile of the mass absorbed by the fiber coating with 0.1 µg/mL (0.1 ppm) initial concentration of PAHs aqueous solution. The aqueous phase is stirred at maximum stirring rate; (A) naphthalene; (B) acenaphthene; (C) phenanthrene; (D) chrysene.

significant increase of equilibration time when  $K_H$  is already very low (below 244 atm·cm<sup>3</sup>/mol). However, even though phenanthrene and chrysene do not reach equilibrium at 70 min, a substantial amount has been extracted into the fiber coating. As shown in Figure 12, the sensitivity of the method is better for phenanthrene than for naphthalene after 20 min.

The long equilibration time for compounds with small  $K_H$  and large  $K_{ow}$  can be improved by enhancing convection in both the headspace and the aqueous phase. Figure 13 shows the time profile of naphthalene, acenaphthene, phenanthrene, and chrysene under the maximum stirring rate of the stirrer. Under this rapid stirring, the equilibration time is shortened to about 3 min for naphthalene and to 10 min for acenaphthene. Both phenanthrene and chrysene do not reach the equilibrium in 45 min, but the amount extracted has increased by 15%. The significant reduction in equilibration time of naphthalene and acenaphthene suggests that this high stirring rate not only agitates the aqueous phase well but may also create the convection in the headspace. This result indicates that the headspace SPME method has potential for analysis of semivolatile organic compounds.

Figure 14 shows the single-ion mode MS spectra of a PAH-contaminated sewage sample. The headspace SPME method was used to extract the contaminants from the headspace above the sewage sample with internal standards added for GC/MS analysis. Naphthalene-*d*<sub>8</sub> and phenanthrene-*d*<sub>10</sub> were used as internal standards for naphthalene and anthracene, respectively. The sampling time was 30 min, and the sewage

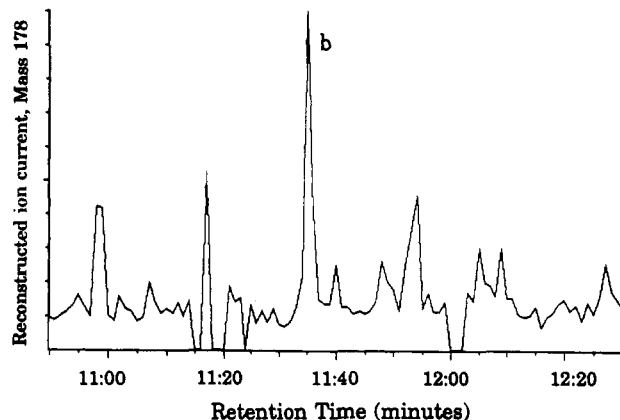
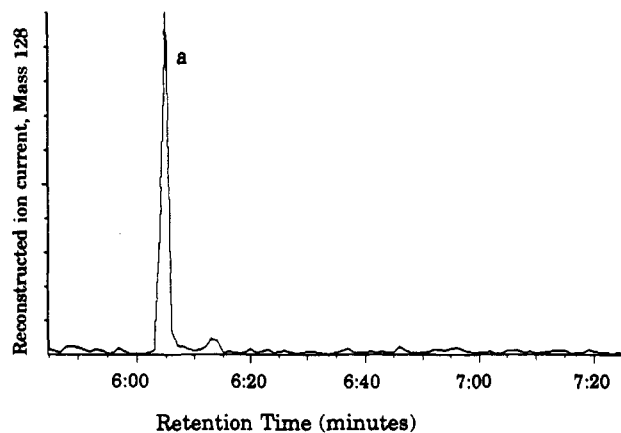


**Figure 14.** Single-ion mode MS spectra of a PAH-contaminated sewage sample: (a) naphthalene and (b) anthracene.

sample was stirred at the maximum rate of the stirrer. From the mass spectra, 2.0 ppb (ng/mL) naphthalene and 0.3 ppb (ng/mL) anthracene were detected in the sewage sample.

The headspace SPME technique cannot only be used to analyze organic contaminants in liquid phase such as water but can also be used to analyze solid samples such as soil. Figure 15 is an example of the headspace SPME analysis of a PAH-contaminated soil sample. The single-ion mode MS spectra clearly indicated the existence of several PAH compounds. Phenanthrene-*d*<sub>10</sub> was used as an internal standard for anthracene and phenanthrene, and chrysene-*d*<sub>12</sub> was used as an internal standard for benz[a]anthracene and chrysene. The headspace of the soil sample was sampled for 30 min, and then the extracted compounds were analyzed by GC/MS. The results gave 17.0 ppm (µg/g) of anthracene, 4.0 ppm (µg/g) of phenanthrene, and 0.23 ppm (µg/g) each for benz[a]anthracene and chrysene.

## CONCLUSIONS

The headspace SPME technique is a new isolation method which can be used to extract a wide range of organic compounds, volatile or semivolatile, from various matrices such as air, water, and soil. This technique also has the ability to concentrate trace compounds from the matrix into the fiber coating since the fiber coating has a very small volume, but the coating [such as poly(dimethylsiloxane)] usually has large coating/matrix partition coefficients for a number of organic compounds. The chemical structure of the coating can be modified to enhance the affinity of target analytes towards the coating. Equation 15 indicates that if the  $K$  value is large, the amount of analyte in the coating can be very significant even when the concentration in the matrix,  $C_0$ , is low. The SPME device not only combines the extraction and concentration together but also directly transfers the absorbed compounds into GC injector. The selective ab-

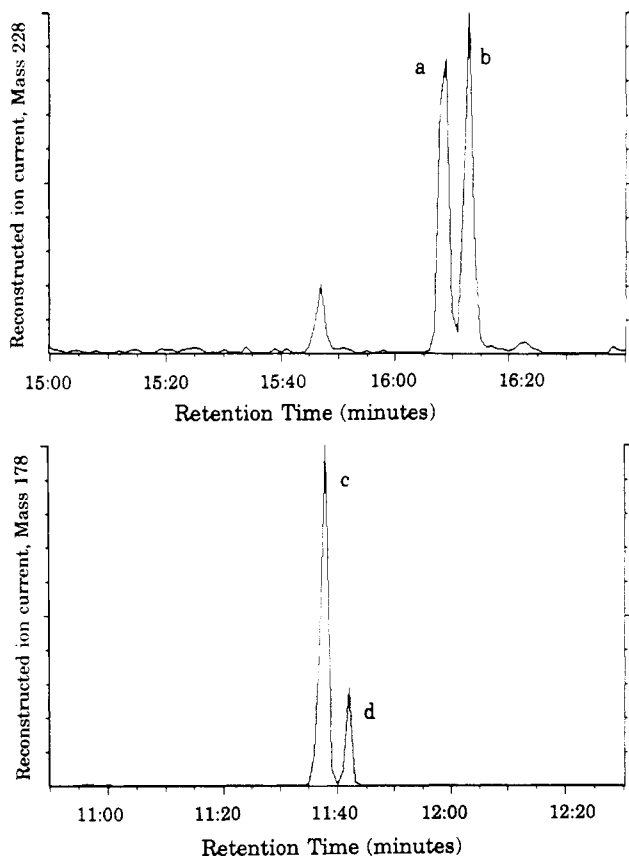


**Figure 15.** Single-ion mode MS spectra of a PAH-contaminated soil sample: (a) benz[a]anthracene, (b) chrysene, (c) anthracene, and (d) phenanthrene.

sorption of the fibre coating prevents a substantial amount of oxygen and moisture from getting into the GC column. These features in the headspace SPME technique provide major advantages over previous headspace techniques.

Compared with direct SPME sampling from aqueous phase, the headspace SPME technique can be used to sample target organic compounds in very complex matrices such as oily or greasy water and human blood. In those cases, the direct SPME sampling will lead to fiber coating enclosed by the grease or impaired by large protein molecules. By sampling from the headspace, these problems can be easily avoided.

For analysis of aqueous samples, the equilibration time in the headspace SPME extraction is controlled by both  $K_1$  and  $K_2$  as discussed in the theoretical section. Since  $K = K_1 K_2$  (refer to eq 14),  $K$  values are often very close to  $K_{ow}$  values, and  $K_2 = K_H/RT$ , it is more practical to say that the equilibration time is controlled by a target organic compound's  $K_{ow}$  and Henry's constant,  $K_H$ . Since values of  $K_{ow}$  and  $K_H$  can be easily found in the literature, it is known well in advance whether or not the headspace SPME method can be used effectively. For compounds that have a very small  $K_H$ , a reasonable equilibration time can still be reached if their  $K_{ow}$  values are small. However, most semivolatile compounds have small  $K_H$  (or  $K_2$ ) values and large  $K_{ow}$  values, like those PAHs listed in Table II, which leads to high extraction sensitivity but long equilibration time. For the poly(dimethylsiloxane) coating used with a magnetic stirring bar, the headspace SPME method can extract compounds very effectively which have a log  $K_{ow}$  value below 4.0 and Henry's constant above 90 atm-cm<sup>3</sup>/mol, as demonstrated in Figure 13. For less

volatile compounds, the development of more efficient techniques can enhance convection of the analytes in both the headspace and the aqueous phase, increase the capacity of the headspace, and thus, reduce the equilibration time. In addition, the extraction process can also be completed without reaching equilibrium and still provide excellent sensitivity if  $K_{ow}$  values of analytes are large.

One possible method to enhance agitation is to spray the aqueous solution into a fine mist before sampling. The fine drops of mist will greatly improve the mass transport of analytes from the aqueous phase to the vapor phase because of a dramatically increased surface to volume ratio as well as the convection in the vapor phase. This method has been suggested in combination with the purge-and-trap<sup>26</sup> but would work much better with the SPME method because of its simplicity. For compounds with high boiling points, sampling the compounds at higher temperatures can also reduce the equilibrium time because Henry's constants increase as temperature increases. The equilibration time for the compounds which have small Henry's constants can be also reduced by using a smaller headspace above the sample. In that case, the concentration gradient in the headspace increases, and it takes less time to diffuse through the headspace. There is another advantage to a smaller headspace as indicated in eq 15: when  $V_3$  decreases, the mass absorbed by the coating increases, thus improving the detection limit. Reducing the headspace would require the changes in the sampling geometry. The present way of sampling, as illustrated in Figure 1a, should be changed, and the polymer-coated fiber put in perpendicular to the vial's axis instead of parallel to it.

The analysis of soil and sludge samples can be quite difficult because of the possible chemisorption of analytes in the solid matrices which limits the recovery of native analytes.<sup>27</sup> This problem has yet to be overcome by many extraction methods. In the headspace SPME method, volatile organic contaminants physically adsorbed by soil can be sampled directly from the headspace. The less volatile compounds or compounds which have strong chemical interactions with the soil can be desorbed by heating the sample to an elevated temperature and then can be sampled by the headspace SPME method. Thermal desorption of organic compounds from the contaminated soil is quite effective for analyzing this difficult category of samples since high temperature can overcome the energy barrier of the chemisorption of analytes on soil.<sup>28</sup> For soil samples containing a wide range of organic compounds, we can use the headspace SPME method to sample more volatile compounds at a lower temperature and sample less volatile compounds at a higher temperature.

Finally, it should be pointed out that though the headspace SPME technique is primarily based on the equilibrium among involved phases, it can also be used to analyze organic compounds without reaching the equilibrium by using internal standards, provided the values of  $K_{ow}$  and  $K_H$  of target compounds are very close to those of their corresponding internal standards.

## ACKNOWLEDGMENT

The authors thank Brian MacGillivray of Wastewater Technology Centre, Burlington, ON, Canada, for providing the PAH-contaminated sewage and soil samples. This work is financially supported by Supelco Inc., Supelco Canada Ltd., and the Natural Sciences and Engineering Research Council of Canada.

(26) Baykut, G.; Voigt, A. *Anal. Chem.* **1992**, *64*, 677.

(27) Alexandrou, N.; Lawrence, M. J.; Pawliszyn, J. *Anal. Chem.* **1992**, *64*, 301.

(28) Robbat, A. J.; Lui, T. Y.; Abraham, B. M. *Anal. Chem.* **1992**, *64*, 1477.